Urszula Ferdek (uferdek@mech.pk.edu.pl)

Faculty of Mechanical Engineering, Cracow University of Technology

The modelling and analysis of shock absorbers
with stroke-dependent damping

Modelowanie i analiza amortyzatora
z tłumieniem zależnym od amplitudy

Abstract

In order to obtain the characteristics of a damping force which depends on the amplitude and frequency of the excitation, a modification to the vehicle shock absorber is proposed in this paper. Within the range of small amplitudes, the 'soft' characteristics improve riding comfort, while within the resonance ranges, the increased damping force provides a higher level of ride safety. A nonlinear model of the system is introduced, taking into account various strategies of oil-flow control. Utilising numerical integration methods, the influence of excitation parameters and constructional parameters on the characteristics of the damper is investigated.

Keywords: hydraulic damper, vehicle suspension, nonlinear vibrations

Streszczenie

W pracy zaproponowano koncepcję amortyzatora samochodowego, którego charakterystyka zależy od amplitudy i częstotliwości wymuszenia. W zakresie małych amplitud charakterystyka miękka poprawia komfort jazdy. W zakresach rezonansowych zwiększona siła tłumienia zapewnia większe bezpieczeństwo jazdy. Opracowano nieliniowy model układu uwzględniający różne strategie sterowania przepływem oleju. Wykorzystując metody numerycznego całkowania, zbadano wpływ parametrów wymuszenia oraz parametrów konstrukcyjnych na charakterystyki tłumika.

Słowa kluczowe: tłumik hydrauliczny, zawieszenie samochodu, nieliniowe drgania

1. Introduction

The problem of the modelling and analysis of hydraulic dampers has been discussed in many papers – this is due to their wide range of applications, especially in the automotive industry. A properly designed damper should meet criteria that are partly contradictory, namely good comfort and high levels of ride safety. Within the range of small amplitudes and high excitation frequencies, a shock absorber should have 'soft' characteristics, and for higher amplitudes, the opposite – 'hard' characteristics. In order to bring together these contradictory requirements, semi-active systems [6], usually magneto-rheological [12], are often applied to adjust the damping force to the conditions of the ride. However, these have a more complicated construction and as a result, they are more expensive both in terms of production and operation. Similar properties of damping characteristics can be obtained with suitably modified passive dampers, e.g. bypass systems [10].

In order to assess the effectiveness of hydraulic dampers, analyses of various vehicle models, e.g. quarter-car or half-car [6, 7, 12] are performed. System responses to harmonic excitations of variable frequencies, impulse or random forces, are most commonly studied. The analysis of a car model requires the introduction of a hydraulic damper model which is relatively simple but properly describes its basic properties, and simultaneously allows the investigation of the influence of essential parameters. Tests of modelling twin-tube dampers [1, 5, 8, 15] and mono-tube dampers [4, 8, 10, 13, 16] are undertaken in many works. These tests mainly differ in their approach to describing the oil flow through the valves.

Alonso & Comas [1] investigated the twin-tube damper model taking into account the cavitation problem and the elasticity of the damper chambers. In order to determine the oil flow rate through the pressure valves, the shim stack blanking off an orifice in a piston is modelling by the stiff plate pressed by a spring. Talbott & Starkey [13] investigated the mono-tube damper, they also modelled the influence of the shim stack pressed by a spring. Flow through orifices covered by a shim stack is much more accurately described by Farjoud et al. [4], who investigated the influence of the shim stack properties on the characteristics of the mono-tube damper.

Benaziz et al. [2] draw attention to the acoustic comfort problem, which depends on valve vibrations. In order to describe valve vibrations, they take into account the inertial and viscoelastic properties of shims and introduce spring-supported movement limiters, which model shim strokes on the piston surface. Ventura [15] determined the frequency characteristics of a quarter-car model with a twin-tube hydraulic damper. The paper includes a comparison of theoretical and experimental pressure diagrams in two chambers of a damper. Funke & Bestle [8] performed the investigation of a mono-tube damper. They investigated the response of the system to harmonic excitations of a limited maximum velocity, assuming – for higher frequencies – appropriately lower excitation amplitudes. Titurus et al. [14] also dealt with the identification problem on the basis of system responses to excitations with a piecewise constant velocity. Witters & Swevers [16] present the black-box identification method of a semi-active mono-tube damper, by means of a neural network. Lee & Moon [10] discuss a model of a displacement-sensitive shock absorber. Depending on the piston displacement, the flow control is realised by the proper configuration of the inner surface of the cylinder.

In the present paper, a model of a hydraulic damper with characteristics dependent on the amplitude and frequency of the excitation is proposed. Numerical analysis of the model shows that the damping force depends on the amplitude and frequency of the excitation. Within the range of small amplitudes and high frequencies, the system behaves like a shock absorber of 'soft' characteristics, which improves driving comfort. Within resonance ranges, the increased damping force provides a higher level of ride safety.

2. Model of variable damping shock absorber

A model of a mono-tube hydraulic shock absorber with a construction similar to the damper presented in papers [3, 9, 11] is presented in Fig.1. There are two chambers filled with oil in the main cylinder: rebound chamber K_1 above the piston; chamber K_2 below the piston. An additional cylinder is rigidly connected to the piston rod and the resiliently attached piston divides this cylinder into two chambers, K_3 and K_4. A floating piston is placed in the main cylinder, separating chamber K_2 (which is filled with oil) from chamber K_5, which is filled with gas under high pressure (2–3 MPa).
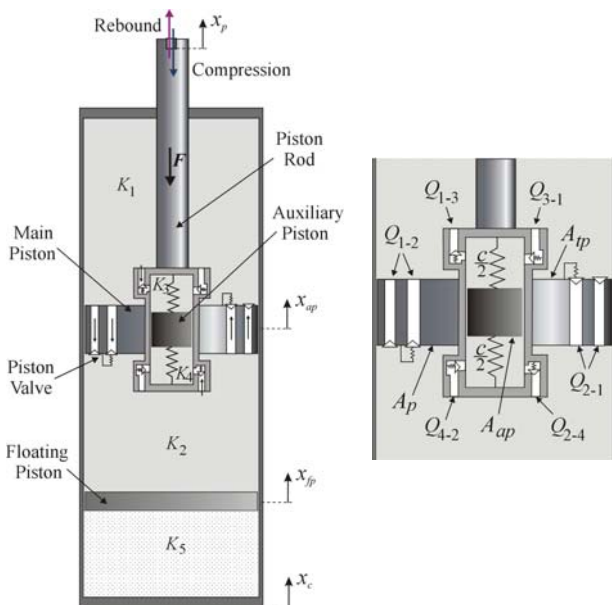
Fig. 1. Damper model

Two phases of piston rod motion are essential in damper operations, namely compression and rebound (expansion). During the compression phase, the piston rod moves down causing a pressure increase in chamber K_2 and the flow of oil into chambers K_1 and K_4. During the rebound process, the oil flows into chambers K_2 and K_3 due to the pressure increase in chamber K_1. Since the orifices in the additional cylinder can be blocked by the auxiliary

piston, the flow of oil into chambers K_3 and K_4 occurs within the limited relative displacement range of the auxiliary piston. The valves are designed so that the flow of oil in the compression and rebound phases occurs through other channels (of different cross-sectional areas), which finally causes asymmetry of the damper characteristics.

The resistance force depends on the resultant pressure force acting on the piston, therefore on the oil pressure in chambers K_1 and K_2. In order to determine these pressures, the processes taking place in the chambers should be considered with special attention directed to the proper description of the flow of oil between the chambers.

The notation used in this paper is as follows:

p_i $(i = 1,..,4)$ – pressures in chambers K_i;

V_i $(i = 1,..,4)$ – current volumes of chambers K_i;

V_{i0} $(i = 1,..,4)$ – initial volumes of chambers K_i (in the equilibrium state);

p_g, V_g, V_{g0} – the gas pressure and the current and initial volumes of chamber K_s;

A_{tp}, A_p – the top and the bottom area of the main piston;

A_{ap} – the area of the additional piston;

x_c – the absolute displacement of the cylinder;

x_p, $x = x_p - x_c$ – the absolute and relative displacements of main piston

x_{fp}, $y = x_{fp} - x_c$ – the absolute and relative displacements of floating piston

x_{ap}, $z = x_{ap} - x_p$ – the absolute and relative displacements of auxiliary piston.

Taking friction force F_{f1} between the main piston and the cylinder into consideration, the damping force can be described as:

$$F = (p_1 - p_0)A_{tp} - (p_2 - p_0)A_p + (p_4 - p_3)A_{ap} + F_{f1}\,\mathrm{sgn}(\dot{x}_p - \dot{x}_c) \qquad (1)$$
$$+ F_{f3}\,\mathrm{sgn}(\dot{x}_p - \dot{x}_{ap}) + c(x_p - x_{ap})$$

where p_0 is the working pressure of the gas. Pressure values p_1 and p_2 depend on all the relative displacements and on the pressures in other damper chambers. In order to determine displacements of the floating piston and the auxiliary piston, the differential equations of the following form need to be solved:

$$m_{fp}\ddot{x}_{fp} = (p_g - p_2)A_p - F_{f2}\,\mathrm{sgn}(\dot{x}_{fp} - \dot{x}_c) \qquad (2)$$

$$m_{ap}\ddot{x}_{ap} = (p_4 - p_3)A_{ap} - cz - F_{f3}\,\mathrm{sgn}(\dot{x}_{ap} - \dot{x}_p) \qquad (3)$$

where m_{fp} is the floating piston mass and m_{ap} is the auxiliary piston mass, and c is the stiffness coefficient of the spring. The friction forces between the floating piston and the cylinder, and also between the auxiliary piston and the additional cylinder, are determined by parameters F_{f2} and F_{f3}. Equations (2–3) describe the vibration of the system around the static equilibrium position. In order to determine gas pressure p_g in chamber K_s, an adiabatic process (or a polytropic process) is usually assumed: $p_g V_g^k = p_0 V_{g0}^k$, where $V_g = V_{g0} + A_p y$. The following formula is then obtained:

$$p_g = p_0 \frac{V_{g0}^{\kappa}}{(V_{g0} + A_p y)^{\kappa}} \tag{4}$$

To determine the oil pressure in chambers K_i ($i = 1, 2, 3, 4$), the following equation can be used:

$$\dot{\rho}_i V_i + \rho_i \dot{V}_i = Q_i \tag{5}$$

where Q_i represents the mass flow rates. Volumes of chambers can be calculated as:

$$V_1 = V_{10} - A_{tp} x \tag{6}$$
$$V_2 = V_{20} + A_p (x - y) \tag{7}$$
$$V_3 = V_{30} - A_{ap} z \tag{8}$$
$$V_4 = V_{40} + A_{ap} z \tag{9}$$

After using the equation describing oil density change ρ_i in chamber K_i:

$$\frac{d\rho_i}{dp_i} = \frac{1}{\beta} \rho_i \tag{10}$$

where β is a bulk modulus, equation (5) can be written as:

$$\dot{p}_i = \frac{\beta}{V_i} \left[\frac{Q_i}{\rho_i} - \dot{V}_i \right] \tag{11}$$

The oil density in the corresponding chamber can be determined directly from the definition $\rho_I = m_i / V_i$ after solving the following differential equation:

$$\dot{m}_i = Q_i \tag{12}$$

3. Model of servo-valve

The operation of the hydraulic damper mainly depends on the strategies used for the control of the flow of oil, in other words on the functions describing mass flow rates Q_i in the damper model. These flow rates are the sum of the flow rates from the individual bleed orifices and are described as:

$$Q_1 = Q_{21} - Q_{12} + Q_{31} - Q_{13} \tag{13}$$

$$Q_2 = Q_{12} - Q_{21} + Q_{42} - Q_{24} \tag{14}$$

$$Q_3 = Q_{13} - Q_{31} \tag{15}$$

$$Q_4 = Q_{24} - Q_{42} \tag{16}$$

where Q_{ji} is the mass flow rate from chamber K_j to chamber K_i. In the case of flow in the reverse direction: $Q_{ji} = 0$ (then $Q_{ij} \neq 0$). In order to determine flow rate Q_{ji}, the turbulent flow is most often assumed [14]:

$$Q_{ji} = C_d A_{ji} \sqrt{2\rho_j (p_j - p_i)} \tag{17}$$

where C_d is the discharge coefficient, while A_{ji} is the effective cross-sectional area of the orifice. Equation (17) is correct for $p_j > p_i$. Area A_{ji} can have constant or variable values, depending on pressures in the respective chambers, or on the relative piston displacements. The damping force depends mainly on the ratio of the total area of the flow channels to the main piston area.

The flow through the valves located in the main piston (Q_{12}, Q_{21}), are considered first. Bleed orifices are usually covered by a stack of circular plates, which are deflecting under the influence of the resultant pressure force and gradually uncovering the orifices. The effective cross-sectional area depends on the geometrical and physical parameters of plates. For simplicity, it is assumed here that in the main piston, apart from the orifices of constantly opened, there are also orifices which are gradually uncovered when the resultant pressure force exceeds the preload force – this occurs when the pressure exceeds the certain critical value s. Let us introduce the function:

$$\theta(p_j - p_i, \sigma, k) = H(p_j - p_i - \sigma)\tanh(p_j - p_i - \sigma)/k \tag{18}$$

where $H()$ is the unit step function, and parameter k characterises the elastic properties of the valve. The maximum value of function q is equal to unity. Effective areas A_{ji} ($j = 1$, $i = 2$ or $j = 2$, $i = 1$) can be written as:

$$A_{ji} = A_p [\alpha_{ji} + \beta_{ji}\theta(p_j - p_i, \sigma_{ji}, k_{ji})] \tag{19}$$

where dimensionless parameters a_{ij} characterise the areas of orifices of constantly opened, and β_{ij} are the maximum areas of orifices covered by plates.

The oil flow into chambers K_3 and K_4 ($Q_{13}, Q_{31}, Q_{24}, Q_{42}$), are now considered. In the proposed damper model, the valves placed in these chambers can be covered by the auxiliary piston, in chamber K_3 for $z > h_1 - r_1$ and in chamber K_4 for $z < -h_2 + r_2$, where distances h_i and r_i, respectively, determine the location of the orifices and their radii. Let us introduce another function:

$$\vartheta(z, h, r) = \begin{cases} 0 & z \geq h + r \\ (h + r - z)/2r & h - r < z < h + r \\ 1 & z < h - r \end{cases} \tag{20}$$

where it is assumed that within the range $(h{-}r, h{+}r)$, the areas of the cross sections are subjected to a linear change. The effective areas in chamber K_3 are described by:

$$A_{ji} = \gamma_{ji} A_p \vartheta(z, h_1, r_1) \theta(p_j - p_i, \sigma_{ji}, k_{ji}) \tag{21}$$

where $j = 1$, $i = 3$ or $j = 3$, $i = 1$, and in chamber K_4 (for $j = 2$, $i = 4$ or $j = 4$, $i = 2$) similarly:

$$A_{ji} = \gamma_{ji} A_p \vartheta(-z, h_2, r_2) \theta(p_j - p_i, \sigma_{ji}, k_{ji}) \tag{22}$$

Dimensionless parameters g_{ij} characterise the maximum cross sectional area value of the orifice. Function q, appearing in equations (21, 22), takes elastic properties of the valves in chambers K_3 and K_4 into account. For $s_{ji} = 0$ (lack of the preliminary down-pressing force) and relatively small values of k_{ji}, the effective area A_{ji} mainly depends on the relative auxiliary piston displacement.

4. Results of the numerical simulations

The basic characteristics of the shock absorber are the dependences of damping forces (1) on the piston displacements and its relative velocity. In order to determine these characteristics, the system of nonlinear differential equations (2, 3) and (11, 12) should be solved for the assumed kinematic excitation $x(t)$. In the case of a damper that is mounted in a car suspension system, the kinematic excitation results from the profile of the road. Such excitation is described by a random function in which a power spectral density is a decreasing frequency function. To determine the damping characteristics, it is more practical to use harmonic excitation, the amplitude of which decreases as frequency increases:

$$x(t) = a \sin \omega t \tag{23}$$

where $\omega a = \omega_1 a_0 = $ const (condition of constant maximum velocity), and $\omega_1 = 2\pi f_1$ is the basic frequency of the vehicle model. For many car models, the first frequency is in the range $f_1 = 1.2\text{-}1.5$ Hz, the second is in the range $f_2 = 12\text{–}18$ Hz. In the range of lower frequencies, vibrations of the so-called spring-supported mass (mainly of the motor-car body) dominate; therefore, this range is responsible for the comfort of the ride. In the second range of higher frequencies, vibrations of non-spring-supported masses are observed, (mainly in the form of wheel vibrations), so this range is important for the safety of the ride.

The values of the characteristic parameters of the shock absorber were determined in the performed simulations. The influence of the parameters determining on the flow of oil between individual chambers $(\alpha_{ij}, \beta_{ij}, \gamma_{ij}, \sigma_{ij})$ and excitation parameters (a, f) was investigated in detail. The following values of parameters were used: $A_p = 10$ cm^2, $A_{tp} = 8$ cm^2, $A_{ap} = 3$ cm^2, $V_{10} = V_{20} = 80$ cm^3, $V_{g0} = 70$ cm^3, $V_{30} = V_{40} = 7.5$ cm^3, $p_0 = 2$ MPa, $\beta = 1.5$ GPa, $\rho_0 = 890$ kgm^{-3}, $m_{fp} = m_{ap} = 0.02$ kg, $c = 500$ Nm^{-1}, $F_{f1} = 10$ N, $F_{f2} = 1$ N, $F_{f3} = 0.1$ N, $k_{12} = k_{21} = 0.6 p_0$, $h_1 = h_2 = h = 2$ cm, $r_1 = r_2 = r = 2$ mm, $C_d = 0.6$, $\kappa = 1.4$. The values of the remaining parameters were changed within certain ranges and they oscillated around the following values: $\alpha_{21} = 0.004$, $\alpha_{12} = 0.002$, $\beta_{21} = 0.016$, $\beta_{12} = 0.008$, $\gamma_{31} = 0.012$, $\gamma_{13} = 0.007$, $\gamma_{24} = \gamma_{42} = 0.012$, $\sigma_{21} = \sigma_{12} = 0.25 p_0$.
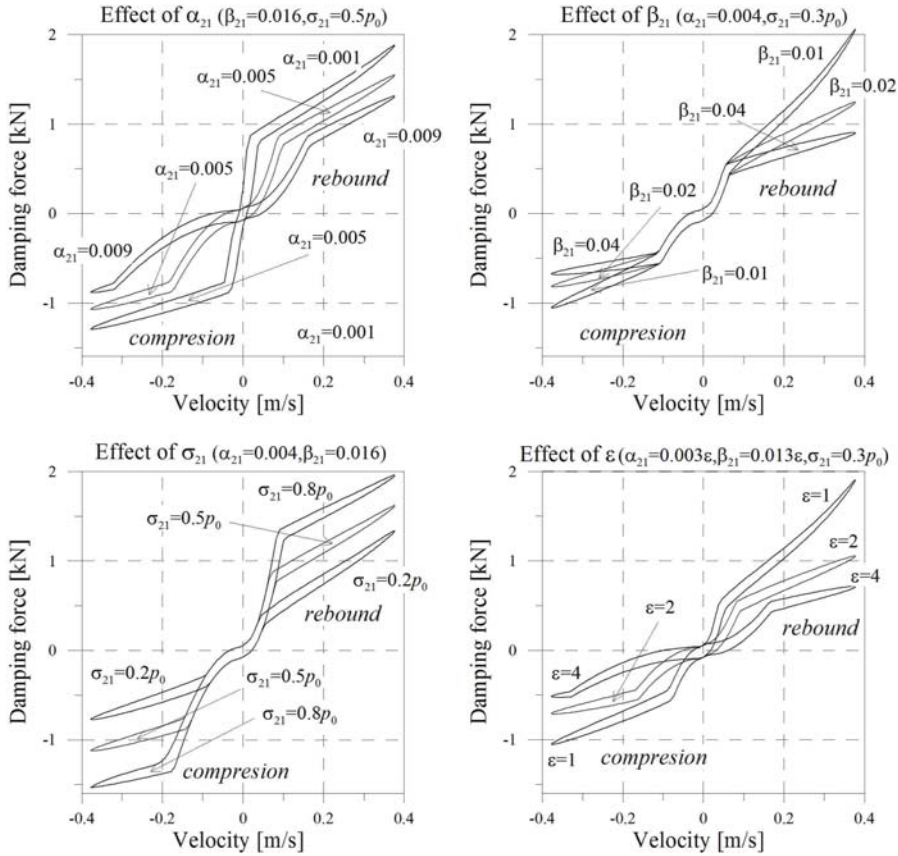
Fig. 2. Influence of valve parameters ($a = 4$ cm, $f = 1.5$ Hz)

The proposed shock absorber, within the ranges of large amplitudes, behaves in a similar fashion to the classic mono-tube damper. In these cases, the flow of oil into the K_3 or K_4 chambers is usually completely or at least partially blocked, and the influence on the damper characteristics is mainly due to the parameters: α_{ij}, β_{ij}, σ_{ij}, $(i = 1,2, j = 2,1)$. These parameters are related to the flow of oil through valves located in the main piston.

The dependence of the damping force on the piston relative velocity for various values of parameters is shown in Fig. 2. In these calculations, it was assumed that: $\alpha_{12} = l\alpha_{21}$, $\beta_{12} = l\beta_{21}$, $l = 0.5$, $\sigma_{21} = \sigma_{12}$, $k_{12} = k_{21} = 0.6p_0$, $\gamma_{31} = 0.012$, $\gamma_{13} = 0.007$, $\gamma_{24} = \gamma_{42} = 0.012$. The damping force characteristics are determined for the excitation amplitude $\alpha = 4$ cm and frequency $f = 1.5$ Hz, this refers to the first resonance range.

The characteristics shown in Fig. 2 are asymmetrical. The resistance force of the damper during the rebound phase is greater than the force in the compression process. Such characteristics are desirable whilst driving over highly uneven surfaces (e.g. driving over a high obstacle). The ratio between the maximum and minimum values of force depends on the ratio of the effective oil flow areas during compression and rebound, that is from the parameter λ.

Parameters α_{21}, α_{12} influence the damping force characteristics within a range of small velocities (Fig. 2a). Within this range, along with the increasing values of parameters α_{21} and α_{12}, the inclination angle of the curve decreases – this shows the dependence of the damping force on the velocity. In turn, with increasing parameters β_{12} and β_{21}, the inclination angle of the curve decreases within the range of high velocities (Fig. 2b). Inflection points occur in diagrams, whose location significantly depends on the value of parameter σ (Fig. 2c). Parameter σ characterises the preload pressure of the shim stack. For larger values of σ, the bleed orifices open later and in effect, the shape of the characteristics changes for higher relative velocities of the piston. Simultaneously, the maximum values of the damping force increase. The damping force decreases along with increases in the effective cross-sectional area of all orifices, that is, with an increasing value of parameter ε (Fig. 2d).
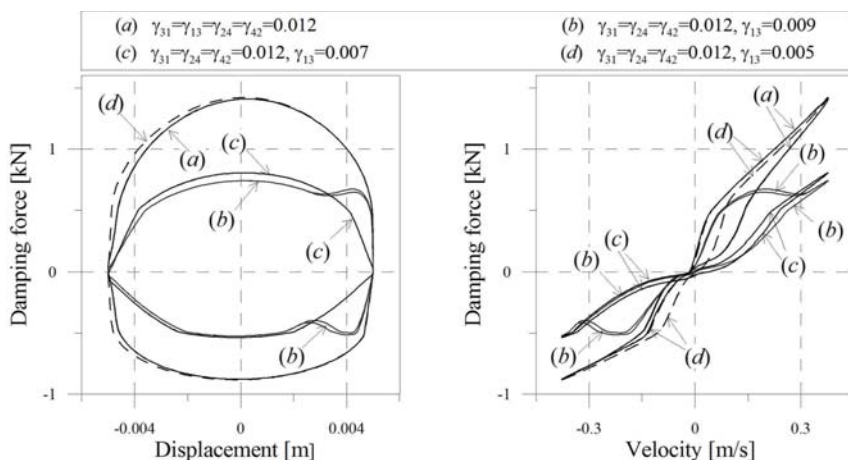
Fig. 3. Damper characteristics $(a = 0.5\ \text{cm}, f = 12\ \text{Hz})$

In the case of high excitation amplitudes, a properly designed damper should has stiff characteristic (usually within the first resonance range) and soft characteristic for small amplitudes (within the second resonance range). Stiff characteristic is obtained when one or more holes in the inner cylinder are blocked (within K_3 or K_4). In order to obtain soft characteristic, the auxiliary piston should move between the valves without blocking them. In other cases, the characteristic change from stiff to soft or inverse. Parameters γ_{31}, γ_{13}, γ_{42} and γ_{24} have a significant influence on the behaviour of the damper. Based on the simulations, it is observed that in the case of symmetrical orifices $\gamma_{31} = \gamma_{13}$ and $\gamma_{24} = \gamma_{42}$, the damper does not work effectively. However, for $\gamma_{24} = \gamma_{42}$, the values of parameters γ_{31} and γ_{13} can be selected so that the characteristics of the damper are soft in the higher frequency range.

The characteristics of the damper in the vicinity of the second resonance (for $a = 5$ mm, $f = 12$ Hz) are shown in Fig. 3 for four parameter values. In the case of curve (a), the valve in chamber K_4 is blocked and the characteristic is stiff; in the case of curve (b), this valve is opened and closed, and the characteristic has the most complicated shape. The best solution is shown in curve (c), where the auxiliary piston moves between the valves, resulting in

a soft characteristics. Curve (d) represents a stiff characteristic, similar to curve (a), but in this case, the valve in chamber K3 is blocked. For smaller frequencies and correspondingly higher amplitudes (within the range of the first resonance, e.g. for f = 1.5 Hz, a = 4 cm), the characteristics are stiff and to a small degree, they depend on parameters γ_{ij}.
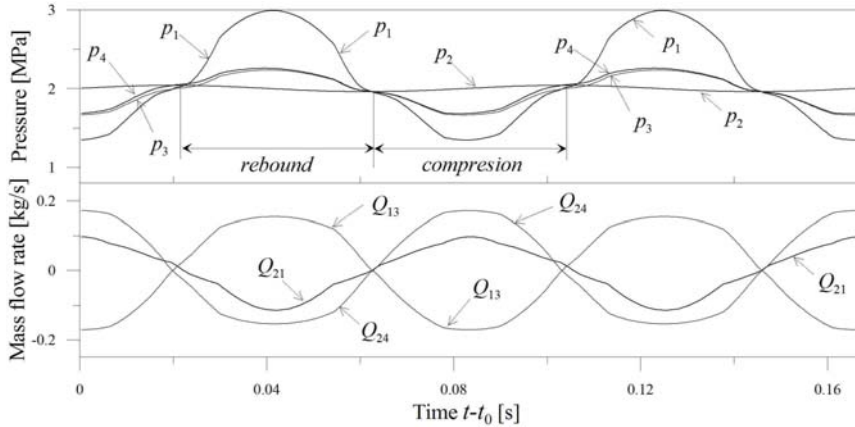
Fig. 4. Pressure time histories and mass flow rates (a = 0.5cm, f = 12Hz)

Diagrams of pressures time histories p_i in chambers K_i ($i = 1,...,4$) and mass flow rates Q_{21}, Q_{13} and Q_{24} corresponding to the characteristics (c) shown in Fig. 3 (for γ_{13} = 0.007), are presented in Fig. 4. The obtained results refer to the state steady of vibration, where t_0 = 2 [s] is the transition period time. Mass flow rates Q_{13} and Q_{24} are almost the same in value. The difference in the sign of these mass flow rates is also easy to explain. In the compression process: Q_{24} > 0 and Q_{13} < 0 (i.e. Q_{31} > 0), this means that the mass of oil flowing to chamber K_4 is approximately equal to the mass of oil flowing out of chamber K_3 (the fluid is compressible). Time histories for pressures p$_3$ and p$_4$ are very similar to each other as a result of the small impact of the spring force and the inertia of the auxiliary piston. Their character is similar to the diagram for pressure p_1. The softest is pressure p_2 – this oscillates around the working pressure. Time intervals corresponding to the compression and rebound are determined by analysing the sign of the relative piston velocity. A decisive influence on the damping force has pressure p_1 in the rebound chamber.

The characteristics of the shock absorber for the excitations satisfying the condition of the same maximum velocity value, i.e. condition fa = const, are shown in Fig. 5. When the excitation frequency increases, its amplitude decreases accordingly. Within the lower frequency range (larger amplitudes), the damping forces are significantly higher (curves (a) and (b) in Fig. 4) than within the higher frequency range. In the case of curves (c) and (d), the auxiliary piston moves in the inner cylinder between the bleed orifices.

The conclusion concerning the characteristics changing from stiff to soft in the higher frequency ranges is correct only under the assumption that the excitation amplitude decreases with increasing frequency. This is the situation which is most often encountered in practice. However, for constant excitation amplitude, the increase of frequency usually results in the

172
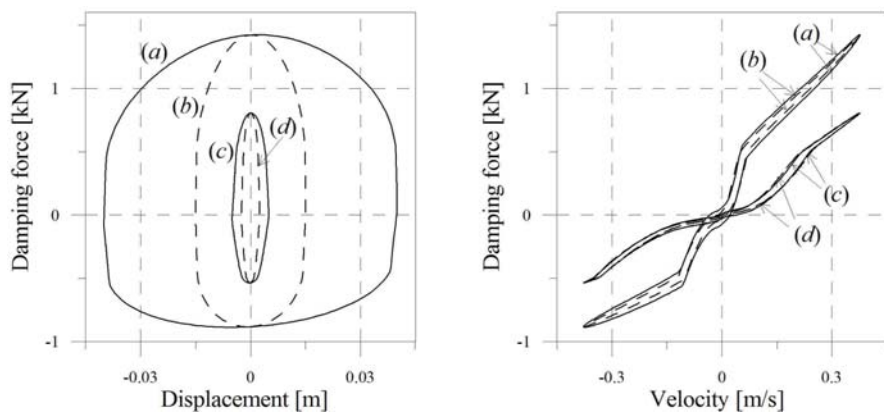
Fig. 5. Damper characteristics: (a) $f = 1.5$ Hz, $a = 40$ mm; (b) $f = 4$ Hz, $a = 15$ mm;
(c) $f = 12$ Hz, $a = 5$ mm; (d) $f = 24$ Hz, $a = 2.5$ mm
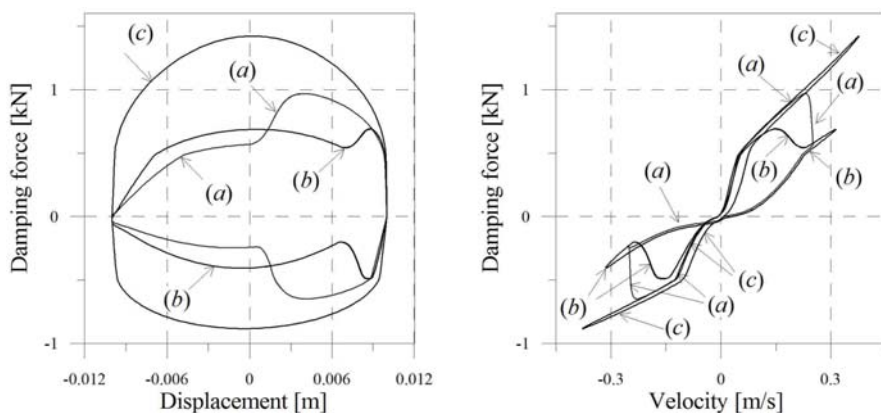
Fig. 6. Damper characteristics ($a = 1$ cm): (a) $f = 4$ Hz; (b) $f = 5$ Hz; (c) $f = 6$ Hz
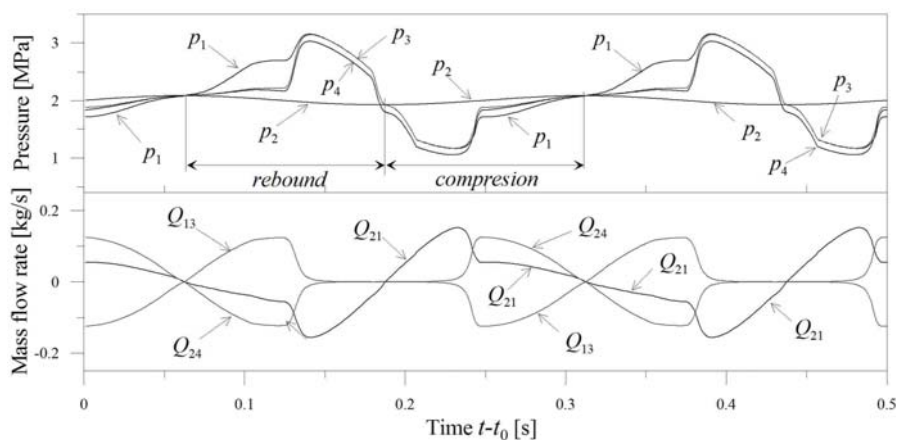
Fig. 7. Pressure time histories and mass flow rates ($a = 1$ cm, $f = 4$ Hz, $g_{24} = g_{42} = g_{31} = 0.012$, $g_{13} = 0.007$

inverse change from soft to stiff characteristics (Fig. 6). This is mainly due to the increase of the maximum values of the relative velocity of the piston.

The diagrams of pressure time histories and mass flow rates corresponding to curve (a) in Fig. 6 are presented in Fig. 7. Most of the conclusions for the analysis of the results shown in Fig. 4 remain valid. Compared Fig. 7 to the previously presented Fig. 4, more rapid changes to pressure p_1 resulting from the jump from the soft branch of characteristics to the stiff branch can be observed. Within time ranges in which $Q_{13} \approx Q_{24} \approx 0$, the valve in chamber K_3 or K_4 is closed.

5. Conclusions

A modified model of a vibration damper with characteristics dependent on the amplitude and frequency of the excitation has been proposed in the present paper. An internal cylinder with auxiliary piston to a classical mono-tube damper has been introduced. The non-linear model description has also been provided – this includes control of the flow of oil between the damper chambers, depending on both pressure and the relative displacement of the piston.

Several numerical simulations were performed and their most important results have been presented in this work. The influence of the constructional parameters of the shock absorber on the damping force characteristics was investigated in detail. The quantitative analysis indicated a significant influence of parameters depending on the geometric and physical properties of the constructional elements of valves in the main piston and in the internal cylinder.

The application of the proposed solution allows the obtaining of a satisfactorily high damping force for large relative displacements of the piston. In such a case, the shock absorber meets the requirements of a 'hard' damper, in doing so, it improves ride safety levels. On the other hand, when the relative displacements are small, the 'soft' damper characteristics provide a high level of ride comfort.

A full analysis of the effectiveness of a damper in a vehicle suspension system requires the development of a vehicle model with the tested damper and the investigation of the influence of its parameters on the indices responsible for both ride safety and ride comfort.

References

[1] Alonso M., Comas Á., *Modelling a twin tube cavitating shock absorber*, Proceedings of the Institution of Mechanical Engineers, Part D: Journal of Automobile Engineering. 220.8, 2006, 1031–1040.

[2] Benaziz M., Nacivet S., Thouverez F., *Nonlinear dynamic analysis of a shock absorber hydraulic spring valve*, Proceedings of ISMA International Conference on Noise and Vibration Engineering, 2012, 3857–3870.

[3] Deferme S., *Stroke dependent bypass*. U.S. Patent No. 6,918,473. 19 Jul. 2005.

[4] Farjoud, Ahmadian M., Craft M., Burke W., *Nonlinear modelling and experimental characterization of hydraulic dampers: effects of shim stack and orifice parameters on damper performance*, Nonlinear Dynamics. 67.2, 2012, 1437–1456.

[5] Ferdek U., Łuczko J., *Modelling and analysis of a twin-tube hydraulic shock absorber*, Journal of Theoretical and Applied Mechanics. 50.2, 2012, 627–638.

[6] Ferdek U., Łuczko J., *Performance comparison of active and semi-active SMC and LQR regulators in a quarter-car model*, Journal of Theoretical and Applied Mechanics. 53.4, 2015, 811–822.

[7] Ferdek U., Łuczko J., *Vibration analysis of a half-car model with semi-active damping*, Journal of Theoretical and Applied Mechanics, 54.2, 2016, 321–332.

[8] Funke T., Bestle D., *Physics-based model of a stroke-dependent shock absorber*, Multibody System Dynamics. 30.2, 2013, 221–232.

[9] Götz O. et al., *Dashpot with amplitude-dependent shock absorption*, U.S. Patent No. 7,441,639. 28 Oct. 2008.

[10] Lee C.T., Moon B.Y., *Simulation and experimental validation of vehicle dynamic characteristics for displacement-sensitive shock absorber using fluid-flow modelling*, Mechanical Systems and Signal Processing. 20.2, 2006, 373–388.

[11] Nowaczyk M., Vochten J.: *Shock absorber with frequency dependent passive valve*, U.S. Patent No. 9,441,700. 13 Sep. 2016.

[12] Prabakar R.S., Sujatha C., Narayanan S., *Optimal semi-active preview control response of a half car vehicle model with magnetorheological damper*, Journal of Sound and Vibration, 326.3, 2009, 400–420.

[13] Talbott M.S., Starkey J., *An experimentally validated physical model of a high-performance mono-tube damper*, SAE Technical Paper, 2002.

[14] Titurus B., Du Bois J., Lieven N., Hansford R., *A method for the identification of hydraulic damper characteristics from steady velocity inputs*, Mechanical Systems and Signal Processing. 24.8, 2010, 2868–2887.

[15] Ventura P., Ferreira C., Neves C., Morais R., Valente A., Reis M.J., *An embedded system to assess the automotive shock absorber condition under vehicle operation*, Sensors, 2008 IEEE. IEEE, 2008, 1210–1213.

[16] Witters M., Swevers J., *Black-box model identification for a continuously variable, electro-hydraulic semi-active damper*, Mechanical Systems and Signal Processing, 24.1, 2010, 4–18.